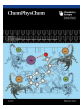

Three in One: The Versatility of Hydrogen Bonding Interaction in Halide Salts with Hydroxy-Functionalized Pyridinium Cations

Loai Al Sheakh,[a] Thomas Niemann,[a] Alexander Villinger,[b] Peter Stange,[a] Dzmitry H. Zaitsau,[a, c] Anne Strate,[a, c] and Ralf Ludwig*[a, c, d]

The paradigm of supramolecular chemistry relies on the delicate balance of noncovalent forces. Here we present a systematic approach for controlling the structural versatility of halide salts by the nature of hydrogen bonding interactions. We synthesized halide salts with hydroxy-functionalized pyridinium cations $[HOC_nPy]^+$ ($n = 2, 3, 4$) and chloride, bromide and iodide anions, which are typically used as precursor material for synthesizing ionic liquids by anion metathesis reaction. The X-ray structures of these omnium halides show two types of hydrogen bonding: 'intra-ionic' H-bonds, wherein the anion interacts with the hydroxy group and the positively charged ring at the same cation, and 'inter-ionic' H-bonds, wherein the anion also interacts with the hydroxy group and the ring system but of different cations. We show that hydrogen bonding is controllable by the length of the hydroxyalkyl chain and the interaction strength of the anion. Some molten halide salts exhibit a third type of hydrogen bonding. IR spectra reveal elusive H-bonds between the OH groups of cations, showing interaction between ions of like charge. They are formed despite the repulsive interaction between the like-charged ions and compete with the favored cation-anion H-bonds. All types of H-bonding are analyzed by quantum chemical methods and the natural bond orbital approach, emphasizing the importance of charge transfer in these interactions. For simple omnium salts, we evidenced three distinct types of hydrogen bonds: Three in one!

The paradigm of supramolecular chemistry relies on the different nature of noncovalent interactions.[1,2] Strong and selective binding between receptor molecules and complementary substrates is controlled by means of various noncovalent intermolecular interaction comprised of electrostatic, hydrogen bonding, van der Waals and donor-acceptor interactions.[3–6] Hydrogen bonding is arguably the most important "type" of such supramolecular phenomena.[7,8] This local and directional interaction is responsible for condensed phase formation, biological self-assembly and molecular recognition.[9,10] Hydrogen bonding is also crucial for properties of salts and ionic liquids, despite the dominating attractive and repulsive Coulomb forces.[11–17]

Herein, we report a systematic study of halide salts consisting of hydroxy-functionalized pyridinium cations and halide anions. These seemingly simple compounds turn out to be complex solids or liquids that exhibit an unusual versatility in hydrogen bonding. The various hydrogen bond structures result from a mélange of intermolecular noncovalent forces in these ionic systems. The structural motifs are controllable by variation of the hydroxyalkyl chain length of the pyridinium cation and the interaction strength of the halide anion, allowing for different strength and directionality of hydrogen bonding. Although the solid or molten omnium salts consist solely of cations and anions, Coulomb interaction is not the driving force for the versatility of local structures. Instead, we demonstrate that three types of hydrogen bonding are present in the solid or liquid states of these halide salts, underlining the importance of the subtle balance of noncovalent interactions. For the first time we report three different types of hydrogen bonding in materials consisting entirely of ions.

In principle, there are several possible modes of interaction between the halide anions and the hydroxy group as well as the ring system of the hydroxy-functionalized pyridinium cations. The delicate competition between the noncovalent intermolecular forces may result in three types of hydrogen bonding. Structures A are characterized by 'intra-ionic' hydrogen bonds (see Scheme 1), wherein the anion interacts with the hydroxy group and the positively charged ring of the same cation. Increasing the length of the hydroxyalkyl chain barely changes the strength of the hydrogen bonds between the anions and the OH groups but results in less favorable interaction of the anion with the pyridinium ring (A1 to A3). Structure B exhibits 'inter-ionic' H-bonds, wherein the anion also interacts with the hydroxy group of the cation but with the

[a] L. Al Sheakh, Dr. T. Niemann, P. Stange, Dr. D. H. Zaitsau, Dr. A. Strate, Prof. Dr. R. Ludwig
Universität Rostock, Institut für Chemie, Abteilung für Physikalische Chemie, Dr.-Lorenz-Weg 2, 18059, Rostock, Germany
E-mail: ralf.ludwig@uni-rostock.de
[b] Dr. A. Villinger
Institut für Chemie, Abteilung für Anorganische Chemie, Universität Rostock, Albert-Einstein-Strasse 3a, 18059 Rostock, Germany
[c] Dr. D. H. Zaitsau, Dr. A. Strate, Prof. Dr. R. Ludwig
Department LL&M, University of Rostock, Albert-Einstein-Str. 25, 18059, Rostock, Germany
[d] Prof. Dr. R. Ludwig
Leibniz-Institut für Katalyse an der Universität Rostock e.V., Albert-Einstein-Str. 29a, 18059 Rostock, Germany

Supporting information for this article is available on the WWW under https://doi.org/10.1002/cphc.202100424

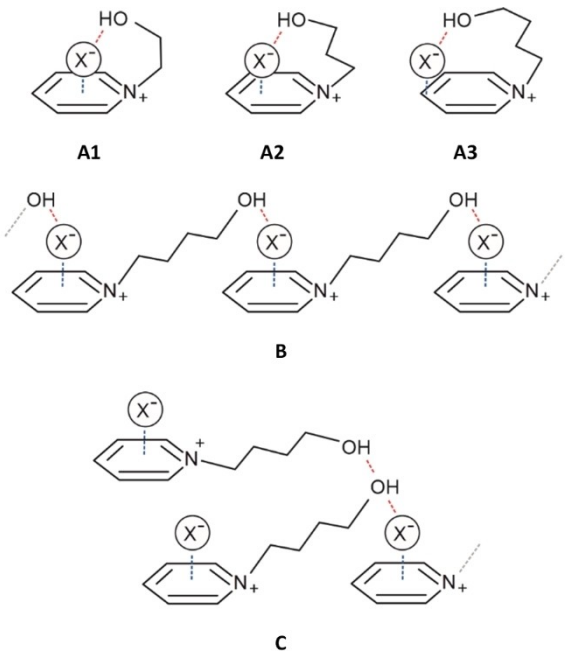

Scheme 1. Possible modes of interaction between the halide anions X^- and the hydroxy group as well as the ring system of the hydroxy-functionalized pyridinium cations $[HOC_nPy]^+$ with $n = 2, 3, 4$. Structures A are characterized by 'intra-ionic' hydrogen bonds, wherein the anion X^- interacts with the hydroxy group and the positively charged ring of the same cation. Increasing the length of the hydroxyalkyl group results in almost remaining strength of the hydrogen bonds between the anions and the OH groups but less favorable interaction of the anion with the pyridinium ring (A1 to A3). Structure B represent 'inter-ionic' H-bonds, wherein the anion also interacts with the hydroxy group and the ring system but of different cations. In structure C, the hydroxy groups of two pydridinium cations form a cooperative H-bond, wherein the OH group on one cation binds to the OH group on the other, which then attaches to the halide anion.

ring system of a different cation. We expect these structures for halide salts with pyridinium cations possessing longer hydroxyalkyl chain lengths ($N_C > 2$). Finally, structure C suggests the possibility that the hydroxy groups of two pydridinium cations form a cooperative H-bond, wherein the OH group on one cation binds to the OH group on the other, which then attaches to the halide anion.

For systematic investigations we synthesized 1-(*n*-hydroxyalkyl)pyridinium halides $[HOC_nPy]X$ including hydroxy-functionalized pyridinium cations $[HOC_nPy]^+$ with $n = 2$, 3, 4 and halide anions $X^- = Cl^-$, Br^-, I^-. Imidazolium, pyridinium, piperidinium or pyrrolidinium halides are typically used as precursor materials for synthesizing ionic liquids by anion metathesis reactions.[18–22] The synthesis of the halide salts follows a literature method and their characterization is described in the Supporting Information (SI). Although being solid at room temperature, most of the synthesized halide salts have low melting points and can be considered as ionic liquids, accepting the somewhat arbitrarily chosen upper melting point limit of 100 °C (see SI).[23] For all halide salts we obtained crystals, which we characterized by X-ray diffraction. Compound $[HOC_4Py]I$ was directly obtained as liquid and showed characteristic behavior of supercooled fluids upon cooling and warming.[22] We studied this compound in the liquid state by means of infrared (IR) spectroscopy, using the OH vibrational mode of the hydroxy functional groups as sensitive probes of hydrogen bonding. We also calculated structures with hydrogen bonding motifs as shown in A, B and C of Scheme 1 by means of density functional theory (DFT) calculations (see SI). The optimized structures, which are close to the observed configurations in the X-ray patterns, were analyzed by the NBO approach for understanding the binding motifs and spectroscopic signatures.[24–33]

Firstly, we discuss the structures of the halide salts $[HOC_2Py]X$ depending on the interaction strength of the chloride, bromide and iodide anions obtained from X-ray analysis (see Table 1) In the $[HOC_2Py]Cl$ and $[HOC_2Py]Br$ halide salts the d(O···Cl) and d(O···Br) hydrogen bond distances are 3.046 Å and 3.202 Å, respectively. In 'intra-ionic' hydrogen bonds, the anion interacts with the hydroxy group of the cation and additionally with the ring system of the same cation (see Figure 1ab, Scheme A1). The strength of the anion-ring interaction is indicated by the close distances between the halide anions and the positively charged range of the ring close to the nitrogen atoms of about d(N···Cl) = 3.813 Å and d(N···Br) = 3.841 Å, respectively. For the $[HOC_2Py]I$ salt we found two H-bond distances d(O···I), namely 3.478 Å and 3.439 Å, suggesting two types of hydrogen bonding with almost identical H-bond strength. The X-ray structures show that the iodide anion allows for both 'intra-ionic' and 'inter-ionic' hydrogen bonds, wherein the anion also interacts with the hydroxy group but with the ring system of a different cation (see Figure 1c, Scheme B). That the 'intra-

Table 1. Intra- and inter-ionic H-bonds distances d(O···X), d(OH···X) (in Å) and H-bond angles ∢(OH···X) (in °) in the halide salts obtained from X-ray structure analysis. Additionally, the distances d(N···X) and d(C···X) (in Å) for the intra-ionic H-bonded structures are given.

Compound	type of H-bond	d(O···X)	d(OH···X)	∢(OH···X)	d(N···X)	d(C···X)
$[HOC_2Py]Cl$	Intra	3.046	2.256	171.7	3.813	3.816
$[HOC_2Py]Br$	Intra	3.202	2.405	173.7	3.841	3.880
$[HOC_2Py]I$	Intra	3.478	2.650	171.3	4.171	4.111
$[HOC_2Py]I$	Inter	3.439	2.651	171.8	5.944	5.953
$[HOC_3Py]Cl$	Inter	3.114	2.291	160.4	–	–
$[HOC_3Py]Br$	Inter	3.289	2.513	169.7	–	–
$[HOC_3Py]Br$	Inter	3.245	2.445	165.5		
$[HOC_3Py]I$	Inter	3.465	2.662	173.3	–	–
$[HOC_4Py]Cl$	Inter	3.058	2.248	173.9	–	–
$[HOC_4Py]Br$	Inter	3.284	2.510	160.9	–	–
$[HOC_4Py]I$	Inter	3.513	2.869	160.4	–	–

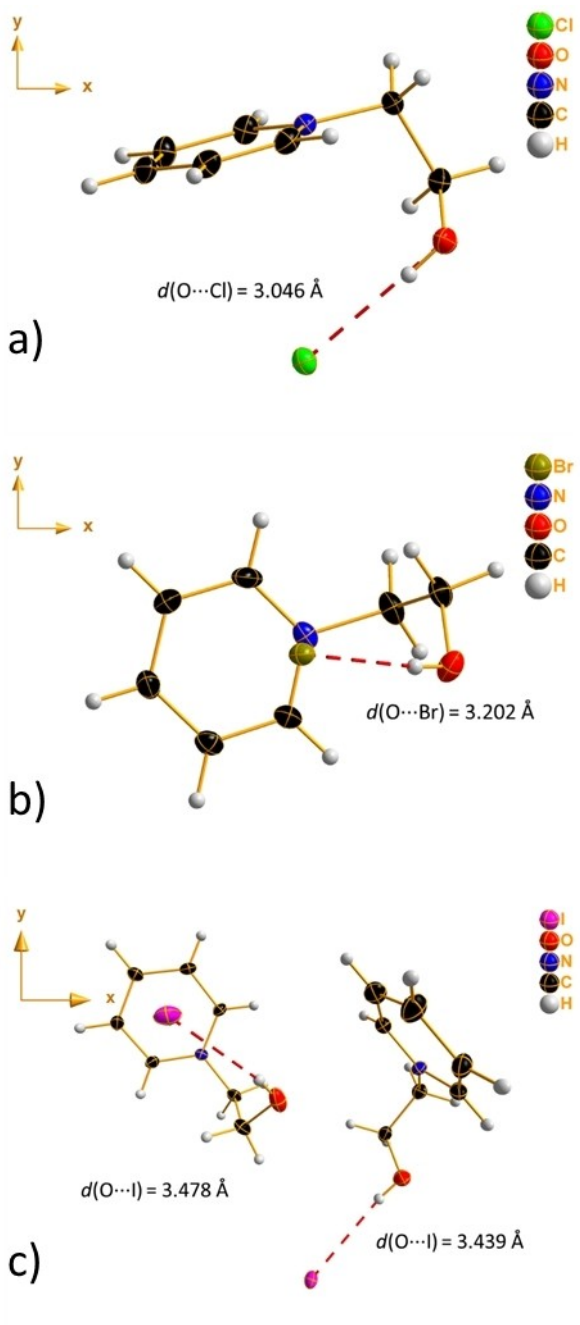

Figure 1. X-ray structures of **a)** [HOC_2Py]Cl, **b)** [HOC_2Py]Br and **c)** [HOC_2Py]I, respectively. Whereas [HOC_2Py]I and [HOC_2Py]Br only possess 'intra-ionic' hydrogen bonds, [HOC_2Py]I shows additional 'inter-ionic' hydrogen bonds and thus both hydrogen bonding features. In the ORTEP representation the atoms are represented by ellipsoids at 50% probability levels. The hydrogen bonds are denoted by dashed line.

ionic' and 'inter-ionic' hydrogen bonds are of similar strength is indicated by the similar H-bond distances *d*(O···X). Thus the iodide anion makes the difference for the short-chained [HOC_2Py]X halide salts, switching from 'intra-ionic' to 'inter-ionic' hydrogen bonds. The 'intra-ionic' hydrogen bond distances d(O···X) increase in the order 3.046 Å, 3.202 Å and 3.478 Å for the chloride, bromide and iodide systems as expected for weaker hydrogen bonding due to decreasing surface charge densities and increasing hydrophobic character of the anions in this sequence. We show in Table 1 that the hydrogen bond angles ∢(O, H, X) range between 160° and 171° for all H-bonds whether they are present in 'intra-ionic' or 'inter-ionic' species.

For the halide salts [HOC_nPy]X with $n>2$ we exclusively observe 'inter-ionic' hydrogen bonds as shown in Figure 1c and illustrated in Scheme B. Due to the longer hydroxyalkyl chain length, the halide anions can no longer form 'intra-ionic' hydrogen bonds. The $X^-\cdots HO^+$ hydrogen bond is still present, but the anion is no longer situated close to the positively charged nitrogen of the same cation. In order to achieve maximum interaction of the anion with the hydroxy groups via hydrogen bonds and with the ring system also, the configuration shown in Scheme B is preferred over those illustrated in Scheme A2 and A3. That the 'intra-ionic' hydrogen bonds are formed in [HOC_2Py]X (Scheme A1), whereas the formation 'inter-ionic' hydrogen bonds is preferred in [HOC_3Py]X and [HOC_4Py]X (Scheme B) halide salts, we rationalize by means of natural bond orbital (NBO) analysis.[28–30] The structures A and B show typical strong $n_L\rightarrow\sigma^*_{OH}$ donor-acceptor interactions between the lone pairs of the halide anions and the OH anti bond orbital of the hydroxy-functionalized pyridinium cations as characterized by the second order stabilization energies $\Delta E^{(2)}_{n\rightarrow\sigma^*}$ and estimated total charge transfers q_{CT} for the $X^-\cdots HO^+$ hydrogen bonds. As shown in Figure 2a, for the example of the calculated halide salts [HOC_nPy]Cl with $n=2$, 3, 4, the sum of the stabilization energies $\Delta E^{(2)}_{n\rightarrow\sigma^*}$ of the 'inter-ionic' H-bonded structures only slightly decreases with increasing hydroxyalkyl chain length due to weaker overall cation-anion interaction. In contrast, the stabilization energies $\Delta E^{(2)}_{n\rightarrow\sigma^*}$ in the 'intra-ionic' structure strongly decrease with increasing hydroxyalkyl chain length. In [HOC_2Py]Cl, the $n_L\rightarrow\sigma^*_{OH}$ interaction is accompanied by additional $n_L\rightarrow\sigma^*_{NC}$ donor-acceptor interaction resulting from the close distance of the anion to the positively charged nitrogen at the pyridinium ring. The sum of both interaction energies allows favoring 'intra-ionic' over 'inter-ionic' hydrogen bonded species for the short-chained cations. In contrast, the $n_L\rightarrow\sigma^*_{NC}$ donor-acceptor interaction almost disappears for [HOC_3Py]Cl and [HOC_4Py]Cl where favorable $n_L\rightarrow\sigma^*_{OH}$ interaction is only possible by pushing the anion away from the positively charged nitrogen (see Scheme A2 and A3). In Figure 2b we show that the overall stabilization energy $\Delta E^{(2)}_{n\rightarrow\sigma^*}$ for halide salts [HOC_2Py]X is not decreasing in the order from chloride to iodide as expected and that instead a slight maximum occurs for [HOC_2Py]Br. We find the regular behavior for $n_L\rightarrow\sigma^*_{OH}$ donor-acceptor interaction for the hydrogen bonds. The deviation from the expected behavior results from the $n_L\rightarrow\sigma^*_{NC}$ interaction between a halide lone pair and the $n_L\rightarrow\sigma^*_{NC}$ anti-bond orbital of the pyridinium ring which is particularly efficient in the [HOC_2Py]Br system. The X-ray structure shows that the bromide anion directly lies above the N–C bond, substantially strengthening this interaction (see Figure 1b).

We have shown that in the solid state, two types of hydrogen bonds are present. Both, 'intra-ionic' and'interionic'

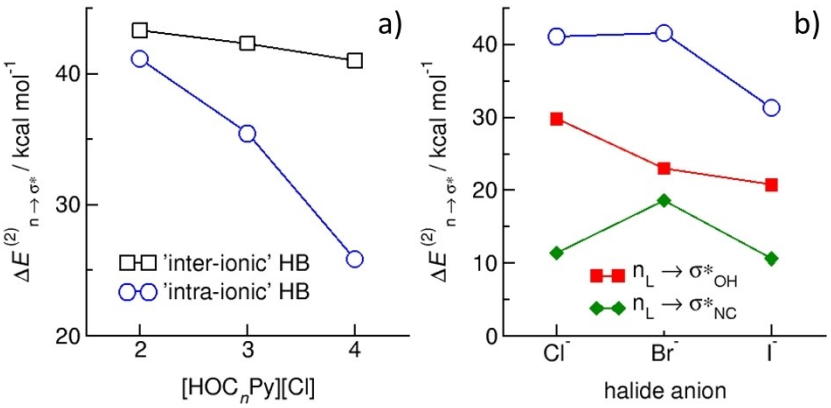

Figure 2. a) Calculated halide salts [HOC$_n$Py]Cl with $n = 2$, 3, 4: the sum of the stabilization energies $\Delta E^{(2)}_{n\rightarrow\sigma^*}$ of the 'inter-ionic' H-bonded structures B (black squares) only slightly decrease with increasing hydroxyalkyl chain length due to weaker overall cation-anion interaction. In contrast, the stabilization energies $\Delta E^{(2)}_{n\rightarrow\sigma^*}$ in the 'intra-ionic' structures (blue circles) strongly decrease with increasing hydroxyalkyl chain length. In [HOC$_2$Py]Cl, the $n_L \rightarrow \sigma^*_{OH}$ interaction is accompanied by additional by $n_L \rightarrow \sigma^*_{NC}$ donor-acceptor interaction resulting from the close distance of the anion to the positively charged nitrogen at the pyridium ring. **b)** Calculated NBO stabilization energies $\Delta E^{(2)}_{n\rightarrow\sigma^*}$ for halide salts [HOC$_2$Py]X with X$^- =$ Cl, Br, I. Against the expectation, the overall stabilization energies of the 'intra-ionic' H-bonded structures (open blue circles) do not continuously decrease in the order Cl, Br to I. NBO analysis provides an explanation. Whereas the stabilization energies $\Delta E^{(2)}_{n\rightarrow\sigma^*}$ for the 'intra-ionic' hydrogen bonds (filled red squares) indeed decrease in the expected way, the overall stabilization energy for [HOC$_2$Py]Br is enhanced by additional $n_L \rightarrow \sigma^*_{NC}$ donor-acceptor interaction resulting from the close distance of the anion to the positively charged nitrogen at the pyridium ring (see also Figure 1b).

hydrogen bonds have in common that they are formed between the hydroxyalkyl group of the pyridinium cation and the halide anion, resulting in hydrogen bonding $^+$OH···X$^-$ enhanced by attractive Coulomb interaction (see Figures 1 and 3). Recently, we reported elusive hydrogen bonds between ions of like charge, observed for hydroxy-functionalized imidazolium and pyridinium cations in ionic liquids by means of infrared (IR) spectroscopy.[34–38] Beside the normal Coulomb-enhanced hydrogen bonds $^+$OH···O$^-$ between cation and anion (c–a), hydrogen bonds $^+$OH…O$^+$ between the positively charged cations (c–c) were observed despite the repulsive Coulomb interaction between ions of like charge. These structural motifs involving H-bonded cationic clusters were observed in the bulk liquid phase by infrared (IR) spectroscopy and in the gas phase by cryogenic ion vibrational predissociation (CIVP) spectroscopy.[39–42] We observed that the formation of cationic clusters was enhanced by using polarizable cations with longer hydroxyalkyl chains as well as weakly interacting anions.[38] Thus, for the salts and ionic liquids considered in this study, [HOC$_4$Py]I should be the best candidate for observing cationic cluster formation (see structure C in Scheme 1). As reported for other ILs comprising iodide anions, the liquid can be supercooled, allowing for IR measurements over broad temperature ranges between 373 and 233 K.[22] In Figure 4a, we show the IR spectra in the OH stretch region. We observe broad spectral bands shifting to lower frequencies and changing their shape with decreasing temperature. Unfortunately, the vibrational band describing the hydrogen bonds $^+$OH···X$^-$ covers the broad frequency range known for cationic clusters from 3550 cm^{-1} for (c–c) dimers down to 3400 cm^{-1} for cyclic tetramers. Thus, the (c–c) vibrational modes may be buried under the dominating (c–a) vibrational band absorbance. Because we know that (c–a) hydrogen bonds dominate at higher temperatures and (c–c) hydrogen bonds start to form at lower temperatures, we subtracted the spectrum recorded at 373 K from all the other spectra for 'depletion' of the spectral features stemming from (c–a) hydrogen bonds. The difference spectra in Figure 4b show negative and positive contributions, resulting from $^+$OH···X$^-$ at higher and lower temperatures, respectively. The important feature is the shoulder around 3250 cm^{-1}, significantly enhanced with decreasing temperature. In accord with frequency calculations on (c–a) and (c–c) hydrogen bonding motifs we assigned this band to the OH group not only interacting with the anion but additionally forming a hydrogen bond to the OH of another cation, resulting in (c–c) hydrogen bonding motifs $^+$OH···$^+$OH···X$^-$. Compared to the regular $^+$OH···X$^-$ vibrational mode, this OH frequency is redshifted due to cooperative effects. Charge is transferred from the anion to the OH anti-

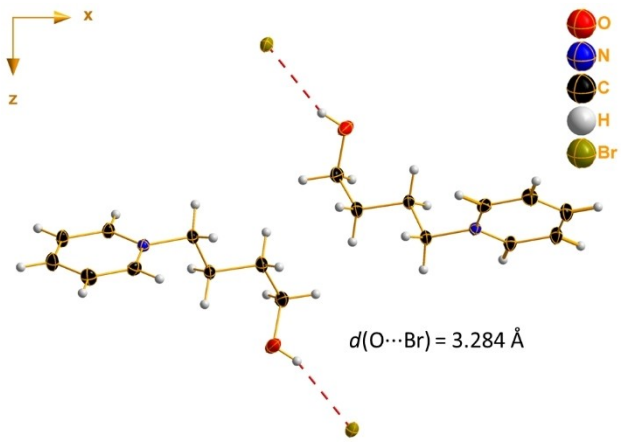

Figure 3. X-ray structure of [HOC$_4$Py]Br. All halide salts [HOC$_n$Py]X with $n > 2$ only exhibit 'inter-ionic' hydrogen bonds. In the ORTEP representation the atoms are represented by ellipsoids at 50% probability levels. The hydrogen bonds are denoted by dashed line.

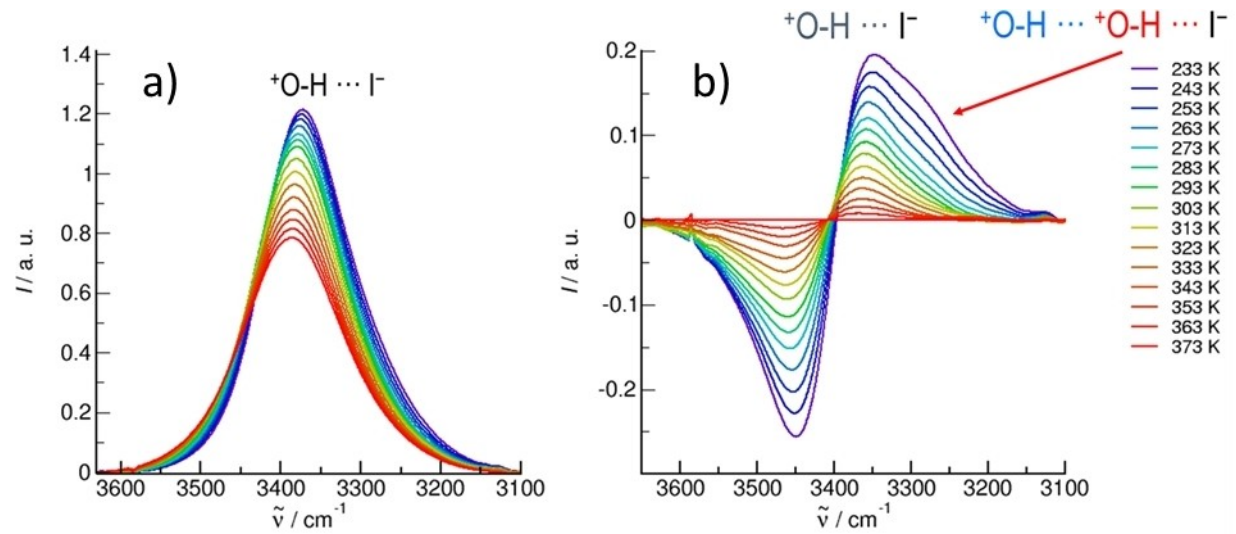

Figure 4. a) IR spectra of the supercooled ionic liquid [HOC_4Py]I in the OH stretch region as a function of temperature between 233 K and 373 K in steps of 10 K. **b)** IR difference spectra of the supercooled ionic liquid [HOC_4Py]I in the OH stretch region as a function of temperature as shown in Figure 4a. From each IR spectrum, we subtracted the spectrum recorded at the highest temperature of 373 K. The shoulder at about 3250 cm^{-1} shows the occurrence of a new vibrational mode at lower temperatures assigned to the OH group interacting with both the anion and a neighboring cation.

bond of the first cation and from there to OH anti-bond of the second cation, enhanced by cooperativity. The $^{+}\underline{OH}\cdots{}^{+}OH\cdots X^{-}$ frequency, expected in the range between 3550 cm^{-1} and 3400 cm^{-1}, is not observed so far. However, subtracting the difference spectrum at 233 K from that at 243 K and that at 223 K from that at 233 K and so on, we obtain decreasing intensity for the (c–a) vibrational band $^{+}OH\cdots X^{-}$ at 3400 cm^{-1} and increasing intensities for the (c–c) vibrational bands $^{+}OH\cdots{}^{+}\underline{OH}\cdots X^{-}$ at 3250 cm^{-1} and $^{+}\underline{OH}\cdots{}^{+}OH\cdots X^{-}$ at 3500 cm^{-1}, respectively (see Figure 5). Thus, we have clear evidence that (c–c–a) hydrogen bonds are formed at the expense of (c–a) hydrogen bonds with decreasing temperature in the low T-range. Recent studies on ionic liquids suggest that we can assign the vibrational frequencies around 3500 cm^{-1} to (c–c) dimers but not large cationic clusters.[34,35] The assignment of the experimentally observed IR vibrational frequencies, ν_{OH}, is supported by the NBO-calculated stabilization energies $\Delta E^{(2)}_{n\rightarrow\sigma^*}$ and charge transfers q_{CT}. In Figure 6, we plot both NBO descriptors versus calculated OH frequencies of the 'intra-ionic' complexes $^{+}OH\cdots X^{-}$ with $X^{-}=Cl^{-}$, Br^{-}, I^{-}. We obtain linear relations between the NBO parameters and the IR frequencies. Stronger hydrogen bonds result in enhanced stabilization energies $\Delta E^{(2)}_{n\rightarrow\sigma^*}$ and charge transfer q_{CT} correlated to further redshifted OH frequencies. The calculated OH frequencies of $^{+}OH\cdots I^{-}$ and $^{+}OH\cdots{}^{+}OH\cdots I^{-}$ complexes fit to this curve and reflect the order of measured frequencies, strongly supporting our assignment and the existence of (c–c) hydrogen bonds in supercooled [HOC_4Py]I.

In this work, we showed that, for a well-suited set of omnium salts comprised of hydroxy-functionalized pyridinium cations and halide anions, two types of hydrogen bonds are present in the solid state: 'intra-ionic' H-bonds, wherein the anion interacts with the hydroxy group and the positively charged pyridinium ring at the same cation, and 'inter-ionic' H-bonds, wherein the anion interacts with the hydroxy group of the cation and the ring system a different cations. The appearance of both types of hydrogen bonds is controllable by the length of the hydroxyalkyl chain and the interaction strength of the anion. The structures were observed in the X-ray patterns of the omnium salts and analyzed by the NBO approach, showing that beside hydrogen bonding, the interaction with the positively charged nitrogen atom in the pyridinium ring plays a role for local structure formation. The

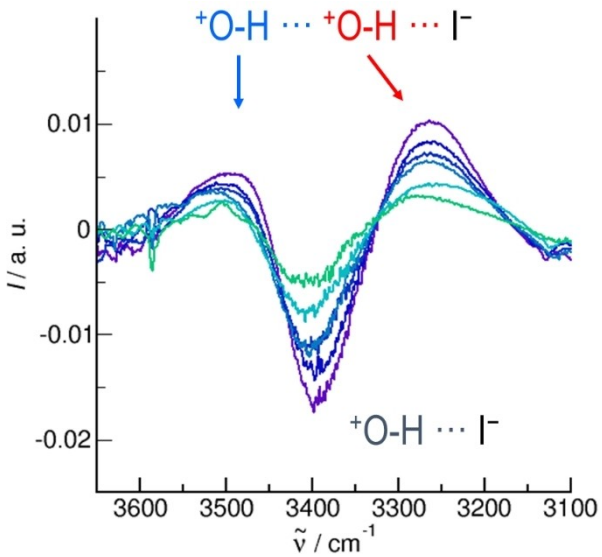

Figure 5. The difference spectra of the next lower temperature are subtracted from the difference spectra shown in Figure 4b. (243 K from 233 K, 253 K from 243 K, etc.). We obtain decreasing intensity for the (c–a) vibrational band $^{+}OH\cdots X^{-}$ at 3400 cm^{-1} and increasing intensities for the (c–c) vibrational bands $^{+}OH\cdots{}^{+}\underline{OH}\cdots X^{-}$ at 3250 cm^{-1} and $^{+}\underline{OH}\cdots{}^{+}OH\cdots X^{-}$ at 3500 cm^{-1}, respectively.

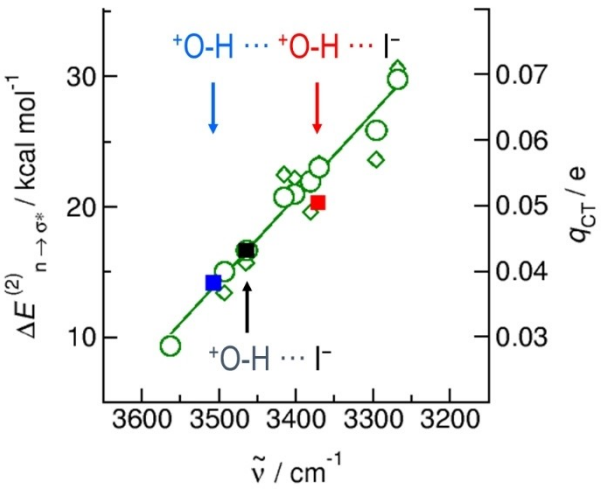

Figure 6. Calculated NBO stabilization energies $\Delta E(2)_{n\rightarrow\sigma^*}$ and charge transfers q_{CT} plotted and versus calculated OH vibrational frequencies for 'intra-ionic' hydrogen bonded complexes $[HOC_nPy]X$ (open green circles and diamonds). The values of the regular $\cdot{}^{+}OH\cdots I^{-}$ (c–a) hydrogen bond (filled black square) and those of the $^{+}OH\cdots{}^{+}\underline{OH}\cdots I^{-}$ hydrogen bond (red square) and the $^{+}\underline{OH}\cdots{}^{+}OH\cdots X^{-}$ hydrogen bond (blue square) in the (c–c–a) species in $[HOC_4Py]I$ are shown for comparison, supporting the assignment of the experimental frequencies.

liquid $[HOC_4Py]I$ with the longest hydroxyalkyl group and the weakest interacting anion can be supercooled. IR difference spectra in the OH stretch region reveal that a third type of hydrogen bonding is possible. At low temperatures, elusive H-bonds between the OH groups of cations show interaction between ions of like charge. They can form despite the repulsive interaction between the like-charged ions and compete with the favored cation-anion H-bonds, which are enhanced by attractive Coulomb interaction. Overall, we present omnium salts with low melting temperatures supporting the importance of the subtle balance between various types intermolecular forces and underlining the specific role of local and directional hydrogen bonds.

Acknowledgement

This work has been funded by the Deutsche Forschungsgemeinschaft (DFG, German Science Foundation – LU-506/12-2) (No. 269854963) and LU-506/14-2 (No. 286149019). Open access funding enabled and organized by Projekt DEAL.

Conflict of Interest

The authors declare no conflict of interest.

Keywords: halide salts · ionic liquids · hydrogen bonding · X-ray crystallography · IR spectroscopy

[1] J.-M. Lehn, *Angew. Chem. Int. Ed. Engl.* **1988**, *27*, 89–112; *Angew. Chem.* **1988**, *100*, 91–116.
[2] J.-M. Lehn, *Science* **1993**, *260*, 1763–1763.
[3] H.-J. Schneider, T. Schiestel, P. Zimmermann, *J. Am. Chem. Soc.* **1992**, *114*, 7698–7703.
[4] M. Albrecht, C. Wessel, M. de Groot, K. Rissanen, A. Lüchow, *J. Am. Chem. Soc.* **2008**, *130*, 4600–4601.
[5] F. Biedermann, H. J. Schneider, *Chem. Rev.* **2016**, *116*, 5216–300.
[6] H. J. Schneider, *Angew. Chem. Int. Ed.* **2009**, *48*, 3924–77.
[7] G. A. Jeffrey, "Introduction to Hydrogen Bonding", Oxford University Press, New York, Oxford, **1997**.
[8] T. Steiner, *Angew. Chem. Int. Ed.* **2002**, *41*, 48; *Angew. Chem.* **2002**, *114*, 50.
[9] G. A. Jeffrey, W. Saenger, "Hydrogen Bonding in Biological Structures"", Springer-Verlag, New York, **1991**.
[10] A. Fersht, "Enzyme Structure and Mechanism", 2nd ed., W. H. Freeman, New York, **1985**.
[11] Ionic Interactions in Natural and Synthetic Macromolecules (A. Ciferri, A. Perico, Eds), **2012** John Wiley & Sons, Inc., p. 35 ff.
[12] H. Weingärtner, *Angew. Chem. Int. Ed.* **2008**, *47*, 654–670; *Angew. Chem.* **2008**, *120*, 664–682.
[13] F. Endres, S. Z. El Abedin, *Phys. Chem. Chem. Phys.* **2006**, *8*, 2101–2116.
[14] T. Welton, *Chem. Rev.* **1999**, *99*, 2077–2084.
[15] N. V. Plechkova, K. R. Seddon, *Chem. Soc. Rev.* **2008**, *37*, 123–150.
[16] K. Fumino, A. Wulf, R. Ludwig, *Angew. Chem.* **2008**, *120*, 8859–8862; *Angew. Chem. Int. Ed.* **2008**, *47*, 8731–8734.
[17] K. Fumino, S. Reimann, R. Ludwig, *Phys. Chem. Chem. Phys.* **2014**, *40*, 21903–21929.
[18] D. Meng, Y. Qiao, X. Wang, W. Wen, S. Zhao, *RSC Adv.* **2018**, *8*, 30180–30185.
[19] T. Niemann, J. Neumann, P. Stange, S. Gärtner, T. G. A. Youngs, D. Paschek, G. G. Warr, R. Atkin, R. Ludwig, *Angew. Chem. Int. Ed.* **2019**, *58*, 12887–12892.
[20] T. Niemann, D. H. Zaitsau, A. Strate, P. Stange, R. Ludwig, *Phys. Chem. Chem. Phys.* **2020**, *22*, 2763–2774.
[21] A. Svatoš, A. B. Attygalle, C. N. Jham, R. T. S. Frighetto, E. F. Vilela, D. Šaman, J. Meinvaldo, *J. Chem. Ecol.* **1996**, *4*, 787–800.
[22] Z. Fei, D. Kuang, D. Zhao, C. Klein, W. H. Ang, S. M. Zakeeruddin, M. Grätzel, P. J. Dyson, *Inorg. Chem.* **2006**, *45*, 10407–10409.
[23] D. MacFarlane, K. R. Seddon, *Aust. J. Chem.* **2007**, *60*, 3–5.
[24] Gaussian 09 (Revision A.02), M. J. Frisch, G. W. Trucks, H. B. Schlegel, G. E. Scuseria, M. A. Robb, J. R. Cheeseman, G. Scalmani, V. Barone, G. A. Petersson, H. Nakatsuji, X. Li, M. Caricato, A. Marenich, J. Bloino, B. G. Janesko, R. Gomperts, B. Mennucci, H. P. Hratchian, J. V. Ortiz, A. F. Izmaylov, J. L. Sonnenberg, D. Williams-Young, F. Ding, F. Lipparini, F. Egidi, J. Goings, B. Peng, A. Petrone, T. Henderson, D. Ranasinghe, V. G. Zakrzewski, J. Gao, N. Rega, G. Zheng, W. Liang, M. Hada, M. Ehara, K. Toyota, R. Fukuda, J. Hasegawa, M. Ishida, T. Nakajima, Y. Honda, O. Kitao, H. Nakai, T. Vreven, K. Throssell, J. A. Montgomery, Jr., J. E. Peralta, F. Ogliaro, M. Bearpark, J. J. Heyd, E. Brothers, K. N. Kudin, V. N. Staroverov, T. Keith, R. Kobayashi, J. Normand, K. Raghavachari, A. Rendell, J. C. Burant, S. S. Iyengar, J. Tomasi, M. Cossi, J. M. Millam, M. Klene, C. Adamo, R. Cammi, J. W. Ochterski, R. L. Martin, K. Morokuma, O. Farkas, J. B. Foresman, D. J. Fox, Gaussian, Inc., Wallingford CT, **2016**.
[25] S. Grimme, J. Antony, S. Ehrlich, H. Krieg, *J. Chem. Phys.* **2010**, *132*, 154104.
[26] S. Ehrlich, J. Moellmann, W. Reckien, T. Bredow, S. Grimme, *ChemPhysChem* **2011**, *12*, 3414–3420.
[27] S. Grimme, A. Jansen, J. G. Brandenburg, C. Bannwarth, *Chem. Rev.* **2016**, *116*, 5105–5154.
[28] ***NBO 6.0***. E. D. Glendening, J. K. Badenhoop, A. E. Reed, J. E. Carpenter, J. A. Bohmann, C. M. Morales, C. R. Landis, F. Weinhold, Theoretical Chemistry Institute, University of Wisconsin, Madison (**2013**).
[29] F. Weinhold, C. R. Landis, *Valency and Bonding A Natural Bond Orbital Donor-Acceptor Perspective*, Cambridge, University Press, Cambridge, **2005**.
[30] F. Weinhold, R. A. Klein, *Mol. Phys.* **2012**, *110*, 565–579.
[31] M. Shukla, N. Srivastava, S. Saha, *J. Mol. Struct.* **2010**, *975*, 349–356.
[32] N. Godbout, D. R. Salahub, J. Andzelm, E. Wimmer, *Can. J. Chem.* **1992**, *70*, 560–71.
[33] C. Sosa, J. Andzelm, B. C. Elkin, E. Wimmer, K. D. Dobbs, D. A. Dixon, *J. Phys. Chem.* **1992**, *96*, 6630–36.
[34] A. Knorr, R. Ludwig, *Sci. Rep.* **2015**, *5*, 17505.
[35] A. Knorr, P. Stange, K. Fumino, F. Weinhold, R. Ludwig, *ChemPhysChem* **2016**, *17*, 458–462.

[36] A. Strate, T. Niemann, P. Stange, D. Michalik, R. Ludwig, *Angew. Chem. Int. Ed.* **2017**, *56*, 496 –500; *Angew. Chem.* **2017**, *129*, 510–514.
[37] T. Niemann, D. Zaitsau, A. Strate, A. Villinger, R. Ludwig, *Sci. Rep.* **2018**, *8*, 14753.
[38] T. Niemann, D. H. Zaitsau, A. Strate, P. Stange, R. Ludwig, *Phys. Chem. Chem. Phys.* **2020**, *22*, 2763–2774.
[39] F. S. Menges, H. J. Zeng, P. J. Kelleher, O. Gorlova, M. A. Johnson, T. Niemann, A. Strate, R. Ludwig, *J. Phys. Chem. Lett.* **2018**, *9*, 2979–2984.
[40] T. Niemann, A. Strate, R. Ludwig, H. J. Zeng, F. S. Menges, M. A. Johnson, *Angew. Chem. Int. Ed.* **2018**, *57*, 15364–15368; *Angew. Chem.* **2018**, *130*, 15590–15594.
[41] T. Niemann, A. Strate, R. Ludwig, H. J. Zeng, F. Menges, M. A. Johnson, *Phys. Chem. Chem. Phys.* **2019**, *21*, 18092–18098.
[42] H. Zeng, F. Menges, M. Johnson, T. Niemann, A. Strate, R. Ludwig, *J. Phys. Chem. Lett.* **2020**, *14*, 683–688.

Manuscript received: June 3, 2021
Revised manuscript received: July 8, 2021
Accepted manuscript online: July 9, 2021
Version of record online: August 4, 2021